ACS OMEGA

http://pubs.acs.org/journal/acsodf

Article

Effects of Zn Addition into ZSM-5 Zeolite on Dehydrocyclization-Cracking of Soybean Oil Using Hierarchical Zeolite-Al_2O_3 Composite-Supported Pt/NiMo Sulfided Catalysts

Atsushi Ishihara,* Shouhei Kanamori, and Tadanori Hashimoto

Cite This: *ACS Omega* 2021, 6, 5509−5517

Read Online

ACCESS | Metrics & More | Article Recommendations | Supporting Information

ABSTRACT: Zn-exchanged ZSM-5-Al_2O_3 (ZA) composite-supported Pt/NiMo (NM) sulfided catalysts were prepared using the conventional kneading method and were tested for dehydrocyclization-cracking of soybean oil. The effects of Zn addition on the activity and selectivity of products were investigated under moderate-pressure conditions of 0.5 and 1.0 MPa H_2 in the temperature range of 420−580 °C. At the temperature 500 °C and higher, most of the sample soybean oil was converted at both the pressures of 0.5 and 1.0 MPa. At 1.0 MPa and 500 °C, the effects of Zn addition appeared and increased the yields of aromatics, while the catalyst without Zn produced larger amounts of products with more than C18. Further, at 0.5 MPa and 580 °C, the gas formation was inhibited in comparison to the cases of 1.0 MPa and the effects of the Zn addition also appeared and increased the yields of aromatics, while the catalyst without Zn produced larger amounts of products with more than C18. The Pt/NM/Zn(122)ZA test catalyst produced more than 63% of liquid fuels in the range C5−C18, and the yield of aromatics was 13%, the maximum value in the present study. The following reaction routes were proposed. The structure of triglyceride is converted by hydrocracking to three molecules of aliphatic acids and propane on the surface PtNiMo sulfide on Al_2O_3 support. The converted aliphatic acids are decomposed through decarboxylation to hydrocarbon fragments, which are further decomposed by cracking on the acid sites of the catalyst, the surface of NiMo sulfide, Al_2O_3, or ZSM-5. Finally, the formed C3 and C4 olefins are transformed to aromatics through the Diels−Alder reaction on the Zn species of ZnZSM-5. On the other hand, although gases were relatively small in amount, aromatic compounds were formed significantly, suggesting that cyclization might directly occur without conversion to gaseous hydrocarbons to some extent.

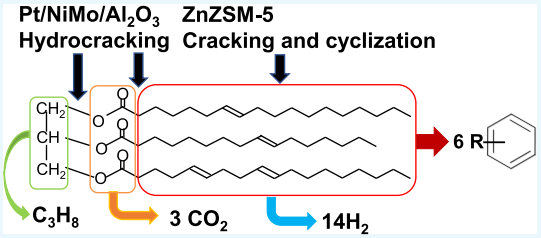

1. INTRODUCTION

While in most of developed countries, more than half of the primary energy source still depends on fossil fuels such as coal, petroleum, and natural gas, it becomes increasingly interesting to use renewable resources year after year. Among the renewable resources, much attention has been paid to carbon-neutral biomass to control recurring environmental issues. Solar energy and wind power of renewable energy sources will not give carbonaceous materials, which can complement the petrochemical industry, while biomass solely provides those carbonaceous matters. It becomes therefore very important to develop process technologies for generating from the biomass most of the matters now provided by the petrochemical industry. Among the biomass feedstocks, fats have such advantageous characteristics of liquids and structures with long alkyl chains that they can be transformed to fuels of gasoline, kerosine, and gas oil; aromatics; and hydrogen. Although transesterification with methanol provides biodiesel fuels, reactants such as glycerol, surplus methanol, and catalysts remain in the final stage of the reaction and have to be removed prior to their utilization.[1−4] Meanwhile, heterogeneous transesterification making fatty acid methyl ester (FAME),[5−7] catalytic cracking making gasoline, propylene, and aromatics for petrochemicals,[8−32] and hydrotreating of fats to biodiesel fuels with high cetane numbers and bio-jet fuels[16−18,33−51] have already been reported during the last decade. Among them, the hydrotreating of fats gives not only vehicle fuels, C3 fraction, and light gas oil with the higher durability for oxidation than that of FAME but also raw materials for petrochemicals, especially aromatics.[52−63] For example, after treatment of fats by ZSM-5 with mesopore and macropore at 300 °C and pressure up to and including 4.0 MPa, hydrotreatment of the oils obtained was performed using NiMo/Al_2O_3 at 340 °C and 4.5 MPa.[52,61] The two-step process using ZSM-5 with a 0.6 cm^3/g pore volume at a high pressure gave 25−29 wt % *n*-paraffin and 8−15 wt % aromatics, whereas aromatics were not given by ZSM-5 with 0.35 cm^3/g pore volume. When deoxygenation of fats was performed using CaO and hydrotalcite at 400 °C in nitrogen

Received: December 1, 2020
Accepted: February 9, 2021
Published: February 18, 2021

https://dx.doi.org/10.1021/acsomega.0c05855
ACS Omega 2021, 6, 5509−5517

atmosphere,[53] more than 80% of hydrocarbon products were obtained. However, the selectivity of aromatics was less than 6%. When sampled vegetable oils were hydrotreated over Pt/Al_2O_3/SAPO-11 at about 380 °C and 30 bar, the product fuels included ca. 15 wt % aromatics.[42,54] Hydrotreating, which gives the stability in products, is performed at a relatively higher hydrogen pressure, and therefore, the yield of aromatics is usually low. In contrast, catalytic cracking of fats gives a higher yield of aromatic compounds.[8,55−59,62,63] For example, catalytic cracking of a fat using HZSM-5 and Mo/HZSM-5 at 650 °C produced more than 50% of aromatic compounds.[55] In another case, the catalytic cracking of a vegetable oil using HZSM-5 (Si/Al = 80) at 450−550 °C in a fixed-bed reactor produced more than 40% of organic liquid products consisting mostly of aromatics.[56] The catalytic cracking gave higher yields of aromatic compounds; however, the unavoidable deactivation occurs in the catalyst used.

It seems that this hydrotreating would have advantages in transforming fats to fuels, and thus we used various types of zeolites in catalyst preparation to obtain gasoline directly by improving their pore structure and acidity at the hydrogen pressure as high as 3.0 MPa.[33] In the course of our study, hydrotreating of fats was performed under the following conditions: hydrogen pressures lower than 1.0 MPa and temperatures higher than 500 °C, which, however, were not common for hydrotreating and hydrocracking. This dehydrocyclization-cracking of fats is hypothetically drawn in the table of contents (TOC), where the catalysts used were the ZSM-5-Al_2O_3 (ZA) composite-supported Pt/NiMo (NM) sulfide catalysts with hierarchical structure, and a gasoline fraction including significant amounts of aromatics is obtained.[64] In this TOC, a molecule of fat includes four double bonds in alkyl long chains, which are assumed to yield 6 molecules of aromatics, 3 molecules of CO_2, 1 molecule of C_3H_8, and 14 molecules of hydrogen. In this scheme, about 7 m^3 of gaseous hydrogen could be prepared from 18 L of fat. However, the composite-supported zeolite catalysts did not produce hydrogen while fat was completely hydrocracked with 1 wt % Pt at 1.0 MPa of hydrogen and 580 °C; 12% of aromatics was obtained at 580 °C when K- and Na-added aluminas and HZSM-5 were mixed, and Pt and NiMo sulfides were supported.[64] Further, β-zeolite-Al_2O_3 composite-supported Pt/NiMo sulfide catalysts yielded aromatics even at 0.5 MPa of hydrogen.[65] On the other hand, it is known that the addition of Zn to zeolites could improve the formation of aromatics in the reforming of saturated hydrocarbons, as our research group has reported recently the precise reaction route from *n*-pentane to BTX on Zn-promoted ZSM-5.[66]

In this reported study, the dehydrocyclization-cracking of soybean oil using Zn-exchanged ZSM-5-Al_2O_3 composite-supported Pt/NiMo sulfide catalysts was performed at a low hydrogen pressure of 0.5 MPa and the effects of Zn addition on the conversion of soybean oil and the formation of aromatics were investigated. Although the effect of the addition of Zn to ZSM-5 on the reaction remains unknown, it was found in the present study that the metal sulfide catalysts could convert soybean oil to valuable fuels and aromatics even at a low pressure 0.5 MPa hydrogen and a higher temperature of 580 °C and also that the addition of Zn would increase aromatics yields.

2. RESULTS AND DISCUSSION

2.1. X-Ray Diffraction (XRD) Patterns for Crystal Structures and N_2 Adsorption and Desorption Measurement for Pore Structures of Pt/NiMo/ZnZSM-5-Al_2O_3 Composite Catalysts. The XRD patterns of the test catalysts before use are shown in Figure 1, where characteristic signals

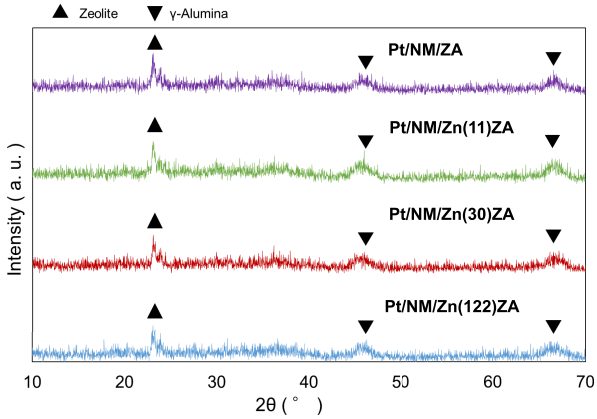

Figure 1. XRD patterns of Pt/NM/ZnZSM-5-Al_2O_3 composite catalysts.

for the zeolite crystals and Al_2O_3 were observed, while there were no such signals for the metal species. The results indicated that the zeolite crystals were kept in the composite supports and that the metal species of Pt, Mo, and Ni were well dispersed in the zeolite-Al_2O_3 composite catalysts. The amount of Pt addition was lower than those of Mo and Ni, and therefore, it may be difficult to detect the former by XRD. However, 1 wt % Pt would appear as XRD signals if it forms crystals. In contrast, the added amounts of Ni and Mo were large, and therefore, if there were crystals on the catalysts, they would appear as XRD signals. When Ni and Mo sulfides are supported on alumina, it is known that they are dispersed on alumina.[67] On the other hand, when they could not be dispersed on a support, they exactly appeared as XRD signals. When these signals are not detected in XRD, the Ni and Mo sulfides under discussion are likely to be dispersed on alumina. After the reaction, the XRD patterns of all catalysts tested were almost the same, as shown in Figures S1 and S2. These results are consistent with those reported previously,[33,64,65] where the zeolite-Al_2O_3 composites worked as appropriate supports for the molybdenum and nickel species, while the metal anionic species would not be retained on a single zeolite.

Pore structures of the Pt/NiMo/ZnZSM-5-Al_2O_3 composite catalysts were estimated by the Brunauer−Emmett−Teller (BET) and Barrett−Joyner−Halenda (BJH) methods in N_2 adsorption and desorption measurement. Table 1 tabulates the results. As the content of ZSM-5 or ZnZSM-5 was 25 wt %, the effects of these microporous materials on pore structures were rather weak, and the values of BET surface areas and total pore volumes were very close to those obtained by the BJH method. Thus, the above-mentioned catalysts exhibited very similar surface areas and pore volumes, which were characteristic of those of alumina. After the reaction, the pore structures were almost the same as shown in Table S1.

NH_3-temperature-programmed desorption (TPD) profiles and the amount of NH_3 desorbed are shown in Figure 2. One broad peak and a long gradual slope were observed between 200 and 600 °C, indicating that the catalysts analyzed

https://dx.doi.org/10.1021/acsomega.0c05855
ACS Omega 2021, 6, 5509−5517

Table 1. Surface Areas, Pore Volumes, and Pore Diameters by the BET and BJH Methods

				BJH		
catalyst	BET SA[a] (m^2/g)	total PV[a] (cm^3/g)	average PD[a] (nm)	SA[a] (m^2/g)	PV[a] (cm^3/g)	PD[a] peak (nm)
Pt/NM/ZA	217	0.47	8.8	225	0.46	10.6
Pt/NM/Zn(11)ZA	227	0.48	8.5	236	0.47	10.6
Pt/NM/Zn(30)ZA	237	0.48	8.1	205	0.45	10.6
Pt/NM/Zn(122)ZA	225	0.48	8.5	209	0.45	10.6

[a]SA: surface area; PV: pore volume; PD: pore diameter. In catalyst names, N, M, Z, and A indicate Ni, Mo, ZSM-5, and alumina, respectively.

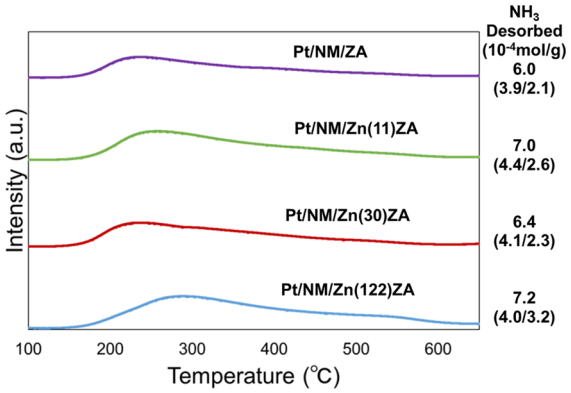

Figure 2. NH_3-TPD curves and amount of NH_3 desorbed in Pt/NM/ZnZSM-5-Al_2O_3 composite catalysts. The total amount of NH_3 desorbed is given on the right-hand side of the figure. The amounts of weak acid sites detected in the range of 100−350 °C (left) and strong acid sites detected in the range of 350−650 °C (right) are given in parentheses.

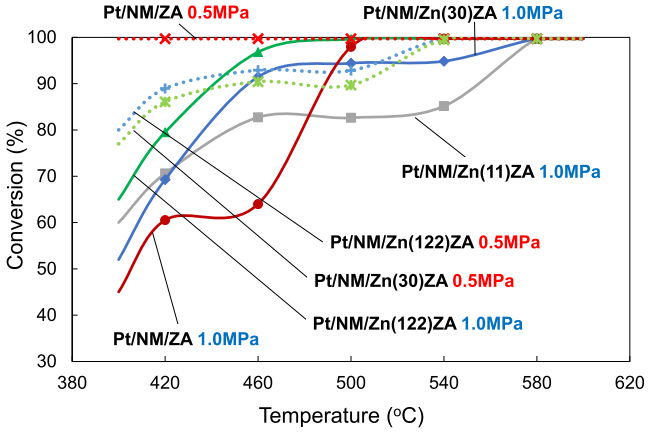

Figure 3. Effect of temperature on the conversion of soybean oil via dehydrocyclization-cracking reaction using Pt/NiMo/ZnZSM-5-Al_2O_3 composite catalysts.

consisted of Al_2O_3, which would make peaks broader. It is likely that, as the amount of NH_3 desorbed was about twice the moles of Al constituting ZSM-5, a significant amount of NH_3 would be adsorbed on the Al_2O_3 component of these catalyst systems.[33,64] In Pt/NM/Zn(122)ZA, the broad peak between 200 and 300 °C was shifted to the higher-temperature range and the shoulder was observed between 500 and 600 °C. When NH_3-TPD data were divided into weak acid sites and strong acid sites at 350 °C, the amount of the strong acid sites tended to increase with increasing amount of Zn added, suggesting that Zn, Si, and Al species would interact with each other and make new acid sites other than those of HZSM-5 itself on Zn sites deposited on the surfaces of ZSM-5.

2.2. Dehydrocyclization-Cracking of Soybean Oil over Pt/NiMo/ZnZSM-5-Al_2O_3 Composite Catalysts. Figure 3 shows the effects of temperature on conversion of soybean oil via dehydrocyclization-cracking reaction using Pt/NiMo/ZnZSM-5-Al_2O_3 composite catalysts. The solid lines indicate the results obtained at 1.0 MPa of hydrogen pressure, and the dotted lines indicate the results at 0.5 MPa of hydrogen. The conversions increased with increasing temperature and reached 100% for all catalysts tested at 580 °C. At a lower temperature of 420 °C, the conversions obtained at 0.5 MPa were higher than those at 1.0 MPa, which would be due to the following reasons: the catalyst surfaces might be reduced at the higher hydrogen pressure, while the activity has not been lost at the higher temperature. Further, it would be mainly because the relative partial pressure of the soybean oil on the catalyst surfaces decreased with hydrogen pressure increasing to 1.0 MPa. As it is assumed that the reaction follows the Langmuir−Hinshelwood rate equation as known in the usual hydrotreating reaction,[67] the retarding term of hydrogen in the denominator of the L−H equation would affect and decrease the rate at the higher pressure of hydrogen. The effects of Zn addition differed depending on the pressure. At the higher hydrogen pressure of 1.0 MPa, the conversion at the lower temperature increased with increasing Zn exchange ratio, suggesting that Zn would activate hydrogen molecules[66] to increase the activity. In contrast, at the lower pressure of 0.5 MPa, the catalyst without Zn exchange revealed the highest conversion at the lower temperature, suggesting that the acid sites of ZSM-5 rather than the reduced Zn sites would directly act as the key active sites.

The reaction profiles of all catalysts are summarized in Tables 2, 3, and S2−S5. These tables tabulate the conversion, branched hydrocarbon-to-straight-chain hydrocarbon (iso-/n-) ratios, research octane number (RON) values for C5−C14, olefin/paraffin ratio (O/P), cetane number, selectivity of gaseous fraction (C1−C4), gasoline fraction (C5−C11), kerosene fraction (C12−C14), diesel fraction (C15−C18), C19 and CO_2 + CO, aromatics yield, and the material balance between feed and product. When the reaction profiles at 500 °C were compared with respect to Table 2 and Figure 4, the conversion approached 100% and the selectivity of gaseous products was kept lower than 40% at 500 °C even at the higher pressure 1.0 MPa. When Zn was added, the fraction with more than C18 (C19 in the tables mentioned above) decreased, the selectivity of gaseous products remained unchanged and the yield of aromatics slightly increased, compared to the catalyst without the addition of Zn.

On the other hand, when the reaction profiles were compared at 580 °C and the lower pressure 0.5 MPa with respect to Table 3 and Figure 4, the conversion reached 100% and the selectivity of gaseous products kept lower, i.e., about 25%. Similar to the cases of the higher pressure 1.0 MPa, with the addition of Zn, the fraction with more than C18 (C19 in

https://dx.doi.org/10.1021/acsomega.0c05855
ACS Omega 2021, 6, 5509−5517

Table 2. Conversion, Iso/n Ratio, RON, Olefin/Paraffin Ratio, Cetane Number, Selectivity of Products, Aromatics Yield, and Material Balance at 1.0 MPa and 500 °C[a]

catalyst	conv. (%)	iso-/n (C5−C14)	RON (C5−C14)	O/P (C2−C3)	CN (C15−C18)			
Pt/NM/ZA	98	1.40	89	0.80	76			
Pt/NM/Zn(11)ZA	83	1.32	84	0.76	72			
Pt/NM/Zn(30)ZA	94	1.39	89	0.80	74			
Pt/NM/Zn(122)ZA	100	1.42	87	0.87	74			
gas (C1−C4) (wt %)	gasoline (C5−C11) (wt %)	kerosene (C12−C14) (wt %)	diesel (C15−C18) (wt %)	C19 (wt %)	CO, CO_2 (wt %)	aroma. yield (wt %)	MB	
36	36	1.8	8.9	10	7.2	10	83	
31	44	3.4	8.9	5.8	7.5	12	88	
38	39	1.8	9.1	4.6	7.7	11	89	
33	44	2.6	9.2	4.6	7.1	11	85	

[a]In catalyst names, N, M, Z, and A indicate Ni, Mo, ZSM-5, and alumina, respectively.

Table 3. Conversion, Iso/n Ratio, RON, Olefin/Paraffin Ratio, Cetane Number, Selectivity of Products, Aromatics Yield, and Material Balance at 0.5 MPa and 580 °C[a]

catalyst	conv. (%)	iso-/n (C5−C14)	RON (C5−C14)	O/P (C2−C3)	CN (C15−C18)			
Pt/NM/ZA	100	0.68	77	0.77	74			
Pt/NM/Zn(30)ZA	100	0.69	77	0.66	73			
Pt/NM/Zn(122)ZA	100	0.76	81	0.66	73			
gas (C1−C4) (wt %)	gasoline (C5−C11) (wt %)	kerosene (C12−C14) (wt %)	diesel (C15−C18) (wt %)	C19 (wt %)	CO, CO_2 (wt %)	aroma. yield (wt %)	MB	
25	45	3.9	8.7	7.9	8.9	9.7	97	
24	47	4.2	8.4	6.6	9.8	11	93	
26	53	4.2	5.9	4.9	6.5	13	100	

[a]In catalyst names, N, M, Z, and A indicate Ni, Mo, ZSM-5, and alumina, respectively.

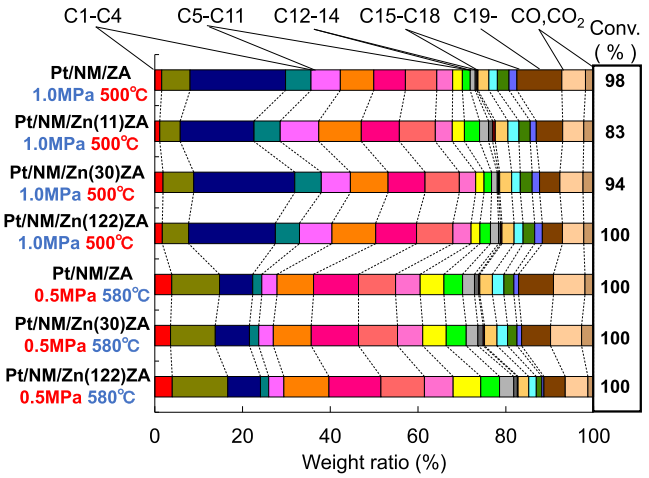

Figure 4. Carbon number distribution of products in dehydrocyclization-cracking reaction of soybean oil using Pt/NiMo/ZnZSM-5-Al_2O_3 composite catalysts.

the tables above) decreased and the yield of aromatics increased, compared to the catalyst without the addition of Zn. The aromatics yield of Pt/NM/Zn(122)ZA at 0.5 MPa and 580 °C was the highest 13% among the catalysts tested. Even at 580 °C, the selectivity of liquid products with C5−C18 was higher at the hydrogen pressure 0.5 MPa than that at 500 °C and 1.0 MPa, reached approximately 60%, and increased with increasing amount of Zn added.

As seen in the general information from all reaction data in Tables S2−S5 for all catalysts, the conversion and the aromatics yield increased and the ratios of iso-/n- and O/P of C2 and C3 decreased with increasing temperature. The decrease in the O/P ratio may be due to the cyclization of C2 and C3 olefins to aromatics.[66] The selectivity of CO and CO_2 tended to increase with increasing temperature. The transportation fuels with C5−C18 were obtained with a selectivity of about 73% at 420 °C and 0.5 MPa of hydrogen in both absence and presence of Zn.

The coke formation in the used catalysts was analyzed by thermogravimetry-differential thermal analysis (TG-DTA) measurement, and the results are shown in Table 4. The

Table 4. Coke Formation Analysis of Used Catalysts by TG-DTA

	H_2 press. (MPa)	200−300 °C (mg)	300−400 °C (mg)	400−500 °C (mg)	500−600 °C (mg)	total[a] (mg)
Pt/NM/ZA	1.0	0.21	0.43	1.41	2.08	4.13 (3.49)
Pt/NM/Zn(11)ZA	1.0	0.23	0.41	0.86	2.44	3.94 (3.30)
Pt/NM/Zn(30)ZA	1.0	0.08	0.17	1.07	2.30	3.62 (3.37)
Pt/NM/Zn(122)ZA	1.0	0.13	0.25	1.19	2.21	3.78 (3.40)
Pt/NM/ZA	0.5	0.27	0.45	1.23	2.18	4.13 (3.41)
Pt/NM/Zn(30)ZA	0.5	0.18	0.30	0.92	2.26	3.65 (3.18)
Pt/NM/Zn(122)ZA	0.5	0.21	0.41	1.25	1.97	3.85 (3.22)

[a]The weight loss at 400−600 °C is shown within parentheses. In catalyst names, N, M, Z, and A indicate Ni, Mo, ZSM-5, and alumina, respectively.

https://dx.doi.org/10.1021/acsomega.0c05855
ACS Omega 2021, 6, 5509−5517

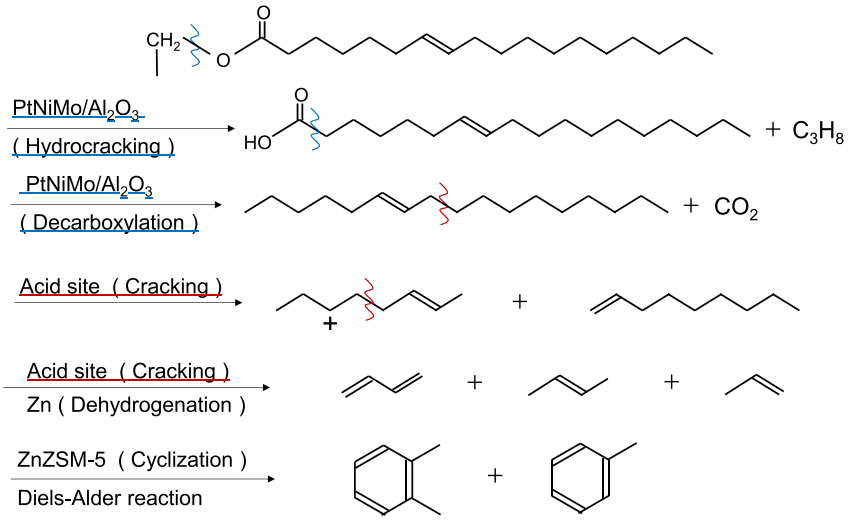

Figure 5. Reaction routes of aromatics formation of soybean oil via dehydrocyclization-cracking using Pt/NiMo/ZnZSM-5-Al_2O_3 composite catalysts.

weight loss at 400−600 °C was attributed to coke, as judged from the TG-DTA curves shown in Figure S3. The coke formation decreased with the addition of Zn, indicating that the presence of Zn would inhibit the coke formation probably because of the promotion of hydrogen transfer near Zn sites of ZSM-5. Further, the coke formation was not affected by the hydrogen pressure between 0.5 and 1.0 MPa, indicating that hydrogen could be provided to carbonaceous fragments even at the pressure as low as 0.5 MPa of hydrogen.

2.3. Reaction Routes in Dehydrocyclization-Cracking Using Pt/NM/ZnZSM-5-Al_2O_3 Composite Catalysts. Figure 5 shows the reaction routes of dehydrocyclization-cracking of soybean oil. The structure of triglyceride would be converted by hydrocracking to three molecules of aliphatic acids and propane on the surface PtNiMo sulfide on Al_2O_3 support. The converted aliphatic acids would be decomposed through decarboxylation to hydrocarbon fragments, which would be further decomposed by cracking on the acid sites of the catalyst. This reaction may be promoted on the surface of NiMo sulfide, Al_2O_3, or ZSM-5, which would be used as acid sites at temperatures of 500 °C and higher. Finally, C3 and C4 olefins would be formed and be transformed to aromatics through Diels−Alder reaction on Zn species of ZnZSM-5. Reduced Zn species may control the size of micropores in ZSM-5 and promote cyclization of olefins and successive dehydrogenation even at both the lower temperature and higher pressure.

In general, the hydrotreatment of a fat in hydrogen atmosphere progresses by hydrodeoxygenation, decarbonylation, and decarboxylation. Among these reactions, decarboxylation and decarbonylation consume less hydrogen. When the reaction progresses through decarboxylation, the yield of CO_2 is expected to reach 15%. The amount summing the formed CO_2 and the CO_2 estimated from the formed CO was lower than 15 wt %, indicating that hydrodeoxygenation would occur to some extent. However, it was thought that more than half of the sample soybean oil would be converted through decarboxylation and decarbonylation using the Pt/NiMo sulfide.[64,65] Further, Zn-exchanged ZSM-5 might affect the formation of CO and CO_2, as it is known that the basic components promote the decarboxylation and decarbonylation.[64,65] In our previous report, the test ZnZSM-5-Al_2O_3 composite catalysts promoted the aromatics formation through dehydrocyclization of *n*-pentane, and it was proposed that dehydrocyclization would progress selectively on reduced Zn sites through Diels−Alder reactions of C4 olefins with ethene, propene, and butene forming benzene, toluene, and xylene, respectively.[66] It is known that hydrocarbons with C1−C5 form aromatics on catalysts including ZSM-5.[66,68−71] In the present study, although gases were relatively small in amount, aromatic compounds were formed significantly, suggesting that cyclization might directly occur without conversion to gaseous hydrocarbons to some extent. As Zn was incorporated into ZSM-5 initially during the preparation of a catalyst, it seems that Zn would act as an active species for cyclization and aromatization of hydrocarbon fragments in the structure of ZSM-5. On the other hand, Pt was supported on the catalyst at the final preparation stage, suggesting that the interaction degree between Zn and Pt could be rather low.

When only NiMo was used without Pt, the activity was rather low. The addition of 0.5 wt % Pt with NiMo was not enough to obtain the activity.[64] Therefore, 1 wt % Pt was used for the catalysts examined. Pt would provide enough hydrogen for a NiMo catalyst to convert the large molecule of a fat. Further, it seems that NiMo sulfide species could initially accelerate the conversion of fat structure to a fatty acid and that the carboxylic acid would successively be decomposed, as shown in Figure 5.

To decrease the consumption of hydrogen, the decarboxylation route is preferred. When CO_2 is formed selectively, however, the reverse reaction with hydrogen may occur forming CO and H_2O. To avoid this reaction, basic compounds were added to the composite supports,[64] which increased decarboxylation and decarbonylation. Generally, basic carriers may reduce aromatics formation because of the decrease in the amounts of acid sites in zeolites. The addition of Zn increased the aromatics formation with the decarbonylation and decarboxylation routes maintained, suggesting that the addition of appropriate substance could achieve simultaneously the formation of aromatics and the decomposition of carboxylic acid without excess consumption of hydrogen.

https://dx.doi.org/10.1021/acsomega.0c05855
ACS Omega 2021, 6, 5509−5517

3. CONCLUSIONS

The test Zn-exchanged ZSM-5-Al_2O_3 composite-supported Pt/NiMo sulfide catalysts increased aromatic compounds compared to the catalysts without Zn and exhibited 11−12% of aromatics yields at 1.0 MPa and 500 °C in the dehydrocyclization of soybean oil. The Zn-exchanged catalysts also increased aromatics yields even at 0.5 MPa and 580 °C, and the Pt/NM/Zn(122)Z(24)60Al catalyst exhibited the low selectivity of gaseous products (26%), while exhibiting the high selectivity of transportation fuels with C5−C18 (63%) and the high yield of aromatics (13%). Zn-exchanged catalysts inhibited the coke formation, compared to the catalysts without Zn.

The Zn-exchanged ZSM-5-Al_2O_3 composite-supported Pt/NiMo sulfide catalyst referred to here can be categorized as a hierarchical type. Although our catalysts may not be the best alternatives for giving aromatic compounds, it is evident that the coexistence of ZSM-5 with very active micropores and Al_2O_3 with mesopores, which can completely maintain Mo anionic species on the surfaces and diffuse the very large carbonaceous molecules such as fats,[67] would bring about the very good performance. Although dehydrocyclization-cracking can be regarded as a technology capable of processing large carbonaceous molecules, it is still required to increase the aromatics selectivity, whereas the more accurate construction of the catalyst materials used would lead to the further development of the hierarchical catalysts as an integral part of the dehydrocyclization-cracking process technology described above.

4. EXPERIMENTAL SECTION

4.1. Material and Catalyst Preparation. The elemental analysis of soybean oil (Wako, extra pure) was C: 76.64%; H: 10.95%; N: 0.30%, and O: balance. Its single components were linoleic acid 50−56%, oleic acid 21−28%, palmitic acid 9−12%, stearic acid 3−5%, and linolenic acid 7−10%. Soybean oil was used without further purification. A zeolite used was ZSM-5 (H type, SiO_2/Al_2O_3 (mol/mol) 24, HSZ-822HOA, Tosoh). Zn-exchanged ZSM-5 was initially prepared by the conventional ion-exchange method using zinc nitrate hexadydrate and aqueous ammonia solution to control pH, and the detailed method was given in the previous paper.[66] Most of Zn added was incorporated into ZSM-5, and the exact amount of Zn was determined by X-ray fluorescence (XRF, Shimadzu EDX-720).

Al_2O_3 (surface area, 250 m^2/g; pore volume, 0.70 cm^3/g; average pore size, 8 nm) was normally used for hydrotreating and was supplied from Nippon Ketjen. Alumina sol (Cataloid AP-1, 70 wt % of Al_2O_3) was used for a binder and was supplied from Shokubai Kasei. The conventional kneading method was used to make hierarchical Zn-exchanged ZSM-5-Al_2O_3 composite supports. ZnZSM-5 (25 wt %), Al_2O_3 (60 wt %), and alumina sol (15 wt %) as Al_2O_3 were mixed with ion-exchanged water and calcined at 500 °C for 3 h in air.[33,64] Metal-loaded catalysts were prepared by the conventional impregnation method using hierarchical composite supports. An aqueous solution of Mo and Ni species including ammonium heptamolybdate tetrahydrate (Nakarai Tesque, $(NH_4)_6Mo_7O_{24}\cdot 4H_2O$) and nickel nitrate hexahydrate (Nakarai Tesque, $Ni(NO_3)_2\cdot 6H_2O$) was used. After impregnation, catalyst samples were dried and calcined at 500 °C for 3 h under air stream. After calcination, catalysts included 16 wt % MoO_3 and 3.3 wt % NiO (Ni/Mo ratio, 0.4). An aqueous solution of $H_2[PtCl_6]\cdot 6H_2O$ was successively used to add 1 wt % Pt to the NiMo catalysts. The name of a composite support was shown with Zn in the top with Zn/Al ratio (mol/mol, Al in ZSM-5) in parentheses, and the abbreviations Z and A for zeolite type ZSM-5 and Al_2O_3, respectively. The name of a metal-supported catalyst was shown as Pt/NM/support name, where N is Ni and M is Mo.

4.2. Characterization of Catalysts and Catalytic Reaction. XRD, N_2 adsorption and desorption, TG-DTA, and NH_3-TPD were measured to characterize the catalysts prepared. The detailed methods have been reported elsewhere.[33,64] XRD patterns were measured to analyze the crystal structure of catalysts using Rigaku Ultima IV under the following conditions: sample, 0.10 g; 2θ = 10−70°; Ni-filtered single-colored Cu Kα_1 radiation (λ = 0.15418 nm); current, 20 mA; voltage, 40 kV; scan speed, 1 °/min; scan mode, continuous; detecting slit, 2/3°; scattering slit, 2/3°; radiation slit, 0.45 mm; present time, 1 s.

To estimate the precise pore structures of catalysts, N_2 adsorption and desorption was measured (BELSORP mini II, Nihon BEL Co. Ltd.). The total surface areas of the catalysts were estimated by the BET method. The surface areas (SA), pore volumes (PV), and pore diameters (PD) of mesopores larger than the pore size of 3.3 nm were estimated by the BJH method. To analyze the changes in the pore structure of catalysts, the spent catalyst was calcined at 500 °C for 12 h to remove residual coke after the reaction was performed. SAs, PVs, and PDs measured by the BET and BJH methods are tabulated in Table 1.

The amounts of NH_3 desorbed for catalysts were measured to evaluate their acidic properties using a gas chromatography-thermal conductivity detector (GC-TCD, Shimadzu GC-8A) under the following conditions: weight of catalyst, 0.04 g; column, 140 °C; injection and detector temperature, 170 °C; current, 100 mA; carrier gas, 10 mL/min; and attenuation.[16] NH_3 was adsorbed at 100 °C by introducing pulses of NH_3 of 1 cc until further adsorption of NH_3 does not occur.

To analyze coke formation, TG-DTA (Shimadzu, DTG-60AH) of spent catalysts was performed under the following conditions: 10 mg of catalyst sample added in an Al pan; temperature range, 25−600 °C, and heating rate, 10 °C/min.

4.3. Dehydrocyclization-Cracking of Soybean Oil Using Pt/NiMo/ZnZSM-5-Al_2O_3 Composite Catalysts. A catalyst (1 g; 600−355 μm: 70 wt %, 355−125 μm: 30 wt %) was packed into a conventional fixed-bed flow reactor (ID, 8 mm; length, 30 cm). Presulfiding of the catalyst was performed under the following conditions: 30 cc/min of 5% H_2S/H_2, 0.1 MPa, 400 °C, 3 h. After cooling, the reactor was pressurized by 0.5 or 1.0 MPa of H_2 and the top of the reactor was preheated by a ribbon heater at around 210 °C. Then, 100% soybean oil was introduced and the temperature was increased at a heating rate of 5 °C/min. The dehydrocyclization-cracking was operated under the following conditions: 0.5 or 1.0 MPa; H_2, 300 mL/min; weight hourly space velocity (WHSV), 6.4 h^{-1}; 420−580 °C. Gas and liquid products including hydrocarbons, CO, and CO_2 were separated in a gas−liquid separator. The volume of gaseous products and weight of liquid products were measured separately. Liquid products with C5−C18 hydrocarbons emerging at 420−580 °C were determined by GC-flame ionization detection (FID). The gaseous products were determined by GC-FID (Shimadzu GC-2014 for gaseous hydrocarbons) and GC-TCD (for CO and CO_2). Diesel fractions of liquid products were determined

https://dx.doi.org/10.1021/acsomega.0c05855
ACS Omega 2021, 6, 5509−5517

by GC-FID (Shimadzu GC-2014), and gasoline fractions of liquid products were determined by GC-FID with PONA solution (Shimadzu GC-2010). The determined gaseous and liquid products were reported in our previous paper.[64] The database in the GC-PONA solution determined more than 95% of the products. The analytical conditions for these GC-FID and GC-TCD were described elsewhere.[33,64]

The product selectivity was estimated in Table 2 according to eq 1

$$\text{product selectivity} = 100 \times (\text{total weights of products in a fraction}) / (W_{gas} + W_{liquid}) \quad (1)$$

where W_{gas} is the weight of gaseous products and W_{liquid} is the weight of liquid products. W_{gas} was estimated from the gas flow rate in the outlet and by the analysis of GC. W_{liquid} was weighed directly. The total product weight in each fraction was estimated by the ratio of the fraction in GC for gas and liquid products and the values of W_{gas} and W_{liquid}.

■ ASSOCIATED CONTENT

Supporting Information

The Supporting Information is available free of charge at https://pubs.acs.org/doi/10.1021/acsomega.0c05855.

Pore structures of used catalysts in N_2 adsorption and desorption measurement (Table S1); conversion, iso/n ratio, RON, olefin/paraffin ratio, cetane number, selectivity of products, aromatics yield, and material balance for Pt/NM/ZA (Table S2); conversion, iso/n ratio, RON, olefin/paraffin ratio, cetane number, selectivity of products, aromatics yield, and material balance for Pt/NM/Zn(11)ZA (Table S3); conversion, iso/n ratio, RON, olefin/paraffin ratio, cetane number, selectivity of products, aromatics yield, and material balance for Pt/NM/Zn(30)ZA (Table S4); conversion, iso/n ratio, RON, olefin/paraffin ratio, cetane number, selectivity of products, aromatics yield, and material balance for Pt/NM/Zn(122)ZA (Table S5); XRD patterns for fresh and used Pt/NM/ZA composite catalysts (Figure S1); XRD patterns of used Pt/NM/ZnZA composite catalysts (Figure S2); and TG-DTA profiles of the used Pt/NM/ZnZA composite catalysts 1.0 and 0.5 MPa (Figure S3) (PDF)

■ AUTHOR INFORMATION

Corresponding Author

Atsushi Ishihara − *Division of Chemistry for Materials, Graduate School of Engineering, Mie University, Tsu, Mie 514-8507, Japan;* orcid.org/0000-0002-6390-8898; Email: ishihara@chem.mie-u.ac.jp

Authors

Shouhei Kanamori − *Division of Chemistry for Materials, Graduate School of Engineering, Mie University, Tsu, Mie 514-8507, Japan*

Tadanori Hashimoto − *Division of Chemistry for Materials, Graduate School of Engineering, Mie University, Tsu, Mie 514-8507, Japan;* orcid.org/0000-0003-2887-7536

Complete contact information is available at: https://pubs.acs.org/10.1021/acsomega.0c05855

Notes

The authors declare no competing financial interest.

■ REFERENCES

(1) Iki, H.; Iguchi, Y. Development of Bio Hydro-fined Diesel (BHD) Technology: Hydrodeoxygenation of Palm Oil and Adaptability of BHD for Diesel Fuel. *J. Jpn. Pet. Inst.* **2012**, *55*, 349−357.

(2) Kubička, D.; Kubickova, I.; Cejka, J. Application of Molecular Sieves in Transformations of Biomass and Biomass-Derived Feedstocks. *Catal. Rev.* **2013**, *55*, 1−78.

(3) Meher, L.; Sagar, D. V.; Naik, S. Technical aspects of Biodiesel Production by transesterification-A Review. *Renewable Sustainable Energy Rev.* **2006**, *10*, 248−268.

(4) Ma, F.; Hanna, M. Biodiesel production: A Review. *Bioresour. Technol.* **1999**, *70*, 1−15.

(5) Semwal, S.; Arora, A.; Badoni, R.; Tuli, D. Biodiesel production using heterogeneous catalysts. *Bioresour. Technol.* **2011**, *102*, 2151−2161.

(6) Yan, S.; Dimaggio, C.; Mahan, S.; Kim, M.; Salley, S.; Ng, K. Advancements in heterogeneous catalysis for biodiesel synthesis. *Top. Catal.* **2010**, *53*, 721−736.

(7) Bournay, L.; Casanave, D.; Delfort, B.; Hillion, G.; Chororge, J. New heterogeneous process for biodiesel production: A way to improve the quarity and the value of the crude glycerin produced by biodiesel plants. *Catal. Today* **2005**, *106*, 190−192.

(8) Ishihara, A.; Kawaraya, D.; Sonthisawate, T.; Kimura, K.; Hashimoto, T.; Nasu, H. Catalytic cracking of soybean oil by hierarchical zeolite containing mesoporous silica-aluminas using a Curie point pyrolyzer. *J. Mol. Catal., A* **2015**, *396*, 310−318.

(9) Busse, O.; Rauchle, K.; Reschetilowski, W. Hydrocracking of Ethyl Laurate on Bifunctional Micro-/Mesoporous Zeolite Catalysts. *ChemSusChem* **2010**, *3*, 563−565.

(10) Al-Sabawi, M.; Chen, J.; Ng, S. Fluid Catalytic Cracking of Biomass-Derived Oils and Their Blends with Petroleum Feedstocks: A Review. *Energy Fuels* **2012**, *26*, 5355−5372.

(11) Tani, H.; Hasegawa, T.; Shimouchi, M.; Asami, K.; Fujimoto, K. Selective catalytic decarboxy-cracking of triglyceride to middle-distillate hydrocarbon. *Catal. Today* **2011**, *164*, 410−414.

(12) Bielansky, P.; Weinert, A.; Schonberger, C.; Reichhold, A. Catalytic conversion of vegetable oils in a continuous FCC pilot plant. *Fuel Process. Technol.* **2011**, *92*, 2305−2311.

(13) Botas, J. A.; Serrano, D. P.; García, A.; Ramos, R. Catalytic conversion of rapeseed oil for the production of raw chemicals, fuels and carbon nanotubes over Ni-modified nanocrystalline and hierarchical ZSM-5. *Appl. Catal., B* **2014**, *145*, 205−215.

(14) Botas, J. A.; Serrano, D. P.; García, A.; de Vicente, J.; Ramos, R. Catalytic conversion of rapeseed oil into raw chemicals and fuels over Ni- and Mo-modified nanocrystalline ZSM-5 zeolite. *Catal. Today* **2012**, *195*, 59−70.

(15) Tsodikov, M. V.; Chistyakov, A. V.; Gubanov, M. A.; Murzin, V. Y.; Bukina, Z. M.; Kolesnichenko, N. V.; Khadzhiev, S. N. Catalytic conversion of rape oil into alkane-aromatic fraction in the presence of Pd-Zn/MFI. *Pet. Chem.* **2013**, *53*, 46−53.

(16) Ishihara, A. Preparation and reactivity of hierarchical catalysts in catalytic cracking. *Fuel Process. Technol.* **2019**, *194*, No. 106116.

(17) Pan, M.; Zheng, J.; Liu, Y.; Ning, W.; Tian, H.; Li, R. Construction and practical application of a novel zeolite catalyst hierarchically cracking of heavy oil. *J. Catal.* **2019**, *369*, 72−85.

(18) Long, F.; Zhai, Q.; Liu, P.; Cao, X.; Jiang, X.; Wang, F.; Wei, L.; Liu, C.; Jiang, J.; Xu, J. Catalytic conversion of triglycerides by metal-based catalysts and subsequent modification of molecular structure by ZSM-5 and Raney Ni for the production of high-value biofuel. *Renewable Energy* **2020**, *157*, 1072−1080.

(19) Gurdeep Singh, H. K.; Yusup, S.; Quitain, A. T.; Abdullah, B.; Ameen, M.; Sasaki, M.; Kida, T.; Cheah, K. W. Biogasoline production from linoleic acid via catalytic cracking over nickel and copper-doped ZSM-5 catalysts. *Environ. Res.* **2020**, *186*, No. 109616.

(20) Singh, O.; Agrawal, A.; Selvaraj, T.; Ghosh, I. K.; Vempatapu, B. P.; Viswanathan, B.; Bal, R.; Sarkar, B. Renewable Aromatics from Tree-Borne Oils (nonedible seed oil) over Zeolite Catalysts Promoted by Transition Metals. *ACS Appl. Mater. Interfaces* **2020**, *12*, 24756−24766.
(21) Xu, G.; Jia, C.; Shi, Z.; Liang, R.; Wu, C.; Liu, H.; Yan, C.; Fan, J.; Hou, H.; Ding, T.; et al. Enhanced catalytic conversion of camelina oil to hydrocarbon fuels over Ni-MCM-41 catalysts. *Sci. Adv. Mater.* **2020**, *12*, 304−311.
(22) Fufachev, E. V.; Weckhuysen, B. M.; Bruijnincx, P. C. A. Tandem catalytic aromatization of volatile fatty acids. *Green Chem.* **2020**, *22*, 3229−3238.
(23) Wang, Y.; Ke, L.; Peng, Y.; Yang, Q.; Du, Z.; Dai, L.; Zhou, N.; Liu, Y.; Fu, G.; Ruan, R.; Xia, D.; Jiang, L. Characteristics of the catalytic fast pyrolysis of vegetable oil soapstock for hydrocarbon-rich fuel. *Energy Convers. Manage.* **2020**, *213*, No. 112860.
(24) Fan, L.; Ruan, R.; Li, J.; Ma, L.; Wang, C.; Zhou, W. Aromatics production from fast co-pyrolysis of lignin and waste cooking oil catalyzed by HZSM-5 zeolite. *Appl. Energy* **2020**, *263*, No. 114629.
(25) Kochaputi, N.; Kongmark, C.; Khemthong, P.; Butburee, T.; Kuboon, S.; Worayingyong, A.; Faungnawakij, K. Catalytic behaviors of supported Cu, Ni, and Co phosphide catalysts for deoxygenation of oleic acid. *Catalysts* **2019**, *9*, No. 715.
(26) Yi, L.; Liu, H.; Li, S.; Li, M.; Wang, G.; Man, G.; Yao, H. Catalytic pyrolysis of biomass wastes over org-CaO/Nano-ZSM-5 to produce aromatics and influence of catalyst properties. *Bioresour. Technol.* **2019**, *294*, No. 122186.
(27) Zou, R.; Wang, Y.; Jiang, L.; Yu, Z.; Zhao, Y.; Wu, Q.; Dai, L.; Ke, L.; Liu, Y.; Ruan, R. Microwave-assisted co-pyrolysis of lignin and waste oil catalyzed by hierarchical ZSM-5/MCM-41 catalyst to produce aromatic hydrocarbons. *Bioresour. Technol.* **2019**, *289*, No. 121609.
(28) Gurdeep Singh, H. K.; Yusup, S.; Quitain, A. T.; Kida, T.; Sasaki, M.; Cheah, K. W.; Ameen, M. Production of gasoline range hydrocarbons from catalytic cracking of linoleic acid over various acidic zeolite catalysts. *Environ. Sci. Pollut. Res.* **2019**, *26*, 34039−34046.
(29) Adamakis, I.-D.; Lazaridis, P. A.; Terzopoulou, E.; Torofias, S.; Valari, M.; Kalaitzi, P.; Rousonikolos, V.; Gkoutzikostas, D.; Zouboulis, A.; Zalidis, G.; Triantafyllidis, K. S. Cultivation, characterization, and properties of *Chlorella vulgaris* microalgae with different lipid contents and effect on fast pyrolysis oil composition. *Environ. Sci. Pollut. Res.* **2018**, *25*, 23018−23032.
(30) Li, T.; Cheng, J.; Zhang, X.; Liu, J.; Huang, R.; Zhou, J. Jet range hydrocarbons converted from microalgal biodiesel over mesoporous zeolite-based catalysts. *Int. J. Hydrogen Energy* **2018**, *43*, 9988−9993.
(31) Xu, J.; Long, F.; Jiang, J.; Li, F.; Zhai, Q.; Wang, F.; Liu, P.; Li, J. Integrated catalytic conversion of waste triglycerides to liquid hydrocarbons for aviation biofuels. *J. Cleaner Prod.* **2019**, *222*, 784−792.
(32) Mohammed, I. Y.; Abakr, A. Y.; Kazi, F. K. In-situ Upgrading of Napier Grass Pyrolysis Vapour Over Microporous and Hierarchical Mesoporous Zeolites. *Waste Biomass Valorization* **2018**, *9*, 1415−1428.
(33) Ishihara, A.; Fukui, N.; Nasu, H.; Hashimoto, T. Hydrocracking of soybean oil using zeolite−alumina composite supported NiMo catalysts. *Fuel* **2014**, *134*, 611−617.
(34) Liu, Y.; Sotelo-Boyás, R.; Murata, K.; Minowa, T.; Sakanishi, K. Hydrotreatment of Vegetable Oils to Produce Bio-Hydrogenated Diesel and Liquefied Petroleum Gas Fuel over Catalysts Containing Sulfided Ni−Mo and Solid Acids. *Energy Fuels* **2011**, *25*, 4675−4685.
(35) Veriansyah, B.; Han, J. Y.; Kim, S. K.; Hong, S.-A.; Kim, Y. J.; Lim, J. S.; Shu, Y.-W.; Oh, S.-G.; Kim, J. Production of renewable diesel by hydroprocessing of soybean oil: Effect of catalysts. *Fuel* **2012**, *94*, 578−585.
(36) Šimáček, P.; Kubička, D.; Kubičková, I.; Homola, F.; Pospíšil, M.; Chudoba, J. Premium quality renewable diesel fuel by hydroprocessing of sunflower oil. *Fuel* **2011**, *90*, 2473−2479.
(37) Sharma, Y. C.; Singh, B.; Upadhyay, S. N. Advancements in development and characterization of biodiesel: A review. *Fuel* **2008**, *87*, 2355−2373.
(38) Huber, G. W.; O'Connor, P.; Corma, A. Processing biomass in conventional oil refineries: Production of high quality diesel by hydrotreating vegetable oils in heavy vacuum oil mixtures. *Appl. Catal., A* **2007**, *329*, 120−129.
(39) Chen, N.; Gong, S.; Shirai, H.; Watanabe, T.; Qian, E. W. Effects of Si/Al ratio and Pt loading on Pt/SAPO-11 catalysts in hydroconversion of Jatropha oil. *Appl. Catal., A* **2013**, *466*, 105−115.
(40) Wang, C.; Liu, Q.; Liu, X.; Yan, L.; Luo, C.; Wang, L.; Wang, B.; Tian, Z. Influence of reaction conditions on one-step hydrotreatment of lipids in the production of iso-alkanes over Pt/SAPO-11. *Chin. J. Catal.* **2013**, *34*, 1128−1138.
(41) Liu, S.; Zhu, Q.; Guan, Q.; He, L.; Li, W. Bio-aviation fuel production from hydroprocessing castor oil promoted by the nickel-based bifunctional catalysts. *Bioresour. Technol.* **2015**, *183*, 93−100.
(42) Rabaev, M.; Landau, M. V.; Vidruk-Nehemya, R.; Koukouliev, V.; Zarchin, R.; Herskowitz, M. Conversion of vegetable oils on Pt/Al_2O_3/SAPO-11 to diesel and jet fuels containing aromatics. *Fuel* **2015**, *161*, 287−294.
(43) Verma, D.; Rana, B. S.; Kumar, R.; Sibi, M. G.; Sinha, A. K. Diesel and aviation kerosene with desired aromatics from hydroprocessing of jatropha oil over hydrogenation catalysts supported on hierarchical mesoporous SAPO-11. *Appl. Catal., A* **2015**, *490*, 108−116.
(44) Li, T.; Cheng, J.; Huang, R.; Zhou, J.; Cen, K. Conversion of waste cooking oil to jet biofuel with nickel-based mesoporous zeolite Y catalyst. *Bioresour. Technol.* **2015**, *197*, 289−294.
(45) Galadima, A.; Muraza, O. Hydrocracking catalysts based on hierarchical zeolites: A recent progress. *J. Ind. Eng. Chem.* **2018**, *61*, 265−280.
(46) Li, F.; Jiang, J.; Liu, P.; Zhai, Q.; Wang, F.; Hse, C.; Xu, J. Catalytic cracking of triglycerides with a base catalyst and modification of pyrolytic oils for production of aviation fuels. *Sustainable Energy Fuels* **2018**, *2*, 1206−1215.
(47) Zhang, Z.; Wang, Q.; Chen, H.; Zhang, X. Hydroconversion of Waste Cooking Oil into Bio-Jet Fuel over a Hierarchical NiMo/USY@Al-SBA-15 Zeolite. *Chem. Eng. Technol.* **2018**, *41*, 590−597.
(48) Dusescu, C.; Juganaru, T.; Bombos, D.; Mihai, O.; Popovici, D. Multilayered catalysts for fatty acid ester hydrotreatment into fuel range hydrocarbons. *C. R. Chim.* **2018**, *21*, 288−302.
(49) Holló, A.; Wollmann, A.; Lonyi, F.; Valyon, J.; Hancsok, J. Alternative Non-Food-Based Diesel Fuels and Base Oils. *Ind. Eng. Chem. Res.* **2018**, *57*, 11843−11851.
(50) Sihombing, J. L.; Pulungan, A. N.; Zubir, M.; Jasmidi; Wibowo, A. A.; Gea, S.; Wirjosentono, B.; Hutapea, Y. A. Conversion of methyl ester fatty acid from rice bran oil into fuel fraction via hydrocracking reaction over zeolite catalyst supported of Ni, Co and Mo metals. *Rasayan J. Chem.* **2019**, *12*, 205−213.
(51) Yeletsky, P. M.; Kukushkin, R. G.; Yakovlev, V. A.; Chen, B. H. Recent advances in one-stage conversion of lipid-based biomass-derived oils into fuel components—aromatics and isomerized alkanes. *Fuel* **2020**, *278*, No. 118255.
(52) Jęczmionek, L.; Krasodomski, W. Hydroconversion of Vegetable Oils Isomerized over ZSM-5: Composition and Properties of Hydroraffinates. *Energy Fuels* **2015**, *29*, 3739−3747.
(53) Romero, M. J. A.; Pizzi, A.; Toscano, G.; Busca, G.; Bosio, B.; Arato, E. Deoxygenation of waste cooking oil and non-edible oil for the production of liquid hydrocarbon biofuels. *Waste Manage.* **2016**, *47*, 62−68.
(54) Rabaev, M.; Landau, M. V.; Vidruk-Nehemya, R.; Goldbourt, A.; Herskowitz, M. Improvement of hydrothermal stability of Pt/SAPO-11 catalyst in hydrodeoxygenation-isomerization-aromatization of vegetable oil. *J. Catal.* **2015**, *332*, 164−176.
(55) Teixeira, C. M.; Frety, R.; Barbosa, C. B. M.; Santos, M. R.; Bruce, E. D.; Pacheco, J. G. A. Mo influence on the kinetics of jatropha oil cracking over Mo/HZSM-5 catalysts. *Catal. Today* **2017**, *279*, 202−208.

https://dx.doi.org/10.1021/acsomega.0c05855
ACS Omega 2021, 6, 5509−5517

(56) Wu, X.; Jiang, P.; Jin, F.; Liu, J.; Zhang, Y.; Zhu, L.; Xia, T.; Shao, K.; Wang, T.; Li, Q. Production of jet fuel range biofuels by catalytic transformation of triglycerides based oils. *Fuel* **2017**, *188*, 205−211.
(57) Ishihara, A.; Tsukamoto, T.; Hashimoto, T.; Nasu, H. Catalytic cracking of soybean oil by ZSM-5 zeolite-containing silicaaluminas with three layered micro-meso-meso-structure. *Catal. Today* **2018**, *303*, 123−129.
(58) Ishihara, A.; Kawaraya, D.; Sonthisawate, T.; Nasu, H.; Hashimoto, T. Preparation and characterization of zeolite-containing silica-aluminas with three layered micro-meso-meso-structure and their reactivity for catalytic cracking of soybean oil using Curie point pyrolyzer. *Fuel Process. Technol.* **2017**, *161*, 8−16.
(59) Sontisawate, T.; Nasu, H.; Hashimoto, T.; Ishihara, A. Catalytic cracking of soybean oil using zeolite-containing microporous and mesoporous mixed catalysts with Curie point pyrolyzer. *J. Jpn. Pet. Inst.* **2016**, *59*, 184−196.
(60) Chistyakov, A. V.; Tsodikov, M. V.; Chudakova, M. V.; Gubanov, M. A.; Zharova, P. A.; Bukina, Z. Y.; Kolesnichenko, N. V.; Gekhman, A. E.; Khadzhiev, S. N. Single-Stage Catalytic Coconversion of Vegetable Oils and Alcohols to the Alkane-Aromatic Hydrocarbon Fraction without Using Molecular Hydrogen. *Pet. Chem.* **2018**, *58*, 258−263.
(61) Jęczmionek, L.; Burnus, Z.; Zak, G.; Ziemianski, L.; Wojtasik, M.; Krasodomski, W.; Stepien, Z.; Rutkowska, M.; Wegrzyn, A. Zeoforming of Triglycerides Can Improve Some Properties of Hydrorefined Vegetable Oil Biocomponents. *Energy Fuels* **2014**, *28*, 7569−7575.
(62) Melero, J. A.; Clavero, M. M.; Calleja, G.; Garcia, A.; Miravalles, R.; Galindo, T. Production of Biofuels via the Catalytic Cracking of Mixtures of Crude Vegetable Oils and Non-edible Animal Fats with Vacuum Gas Oil. *Energy Fuels* **2010**, *24*, 707−717.
(63) Pinto, F.; Varela, F. T.; Goncalves, M.; Neto Andre, R.; Costa, P.; Mendes, B. Production of bio-hydrocarbons by hydrotreating of pomace oil. *Fuel* **2014**, *116*, 84−93.
(64) Ishihara, A.; Ishida, R.; Ogiyama, T.; Nasu, H.; Hashimoto, T. Dehydrocyclization-cracking reaction of soybean oil using zeolite-metal oxide composite-supported PtNiMo sulfided catalysts. *Fuel Process. Technol.* **2017**, *161*, 17−22.
(65) Shirasaki, Y.; Nasu, H.; Hashimoto, T.; Ishihara, A. Effects of types of zeolite and oxide and preparation methods on dehydrocyclization-cracking of soybean oil using hierarchical zeolite-oxide composite-supported Pt/NiMo sulfided catalysts. *Fuel Process. Technol.* **2019**, *194*, No. 106109.
(66) Ishihara, A.; Takai, K.; Hashimoto, T.; Nasu, H. Effects of a Matrix on Formation of Aromatic Compounds by Dehydrocyclization of *n*-Pentane Using ZnZSM-5−Al_2O_3 Composite Catalysts. *ACS Omega* **2020**, *5*, 11160−11166.
(67) Kabe, T.; Ishihara, A.; Qian, W. *Hydrodesulfurization and Hydrodenitrogenation*; Kodansha, Wiley-VCH, 1999; pp 1−374.
(68) Roshanaei, A.; Alavi, S. M. Using two-zone fluidized bed reactor in propane aromatization over Zn/HZSM-5 catalyst. *Fuel Process. Technol.* **2018**, *176*, 197−204.
(69) Wannapakdee, W.; Suttipat, D.; Dugkhuntod, P.; Yutthalekha, T.; Thivasasith, A.; Kidkhunthod, P.; Nokbin, S.; Pengpanich, S.; Limtrakul, J.; Wattanakit, C. Aromatization of C5 hydrocarbons over Ga-modified hierarchical HZSM-5 nanosheets. *Fuel* **2019**, *236*, 1243−1253.
(70) He, P.; Jarvis, J.; Meng, S.; Wang, A.; Kou, S.; Gatip, R.; Yung, M.; Liuc, L.; Song, H. Co-aromatization of methane with olefins: The role of inner pore and external surface catalytic sites. *Appl. Catal., B* **2018**, *234*, 234−246.
(71) Kelkar, S.; Saffron, C. M.; Li, Z.; Kim, S.-S.; Pinavaia, T. M.; Miller, D. J.; Kriegel, R. Aromatics from biomass pyrolysis vapor using a bifunctional mesoporous catalyst. *Green Chem.* **2014**, *16*, 803−812.

https://dx.doi.org/10.1021/acsomega.0c05855
ACS Omega 2021, 6, 5509−5517